Preparation and Characterization of Polypropylene/Clay Nanocomposites with Polypropylene-graft-Maleic Anhydride

Lee Wook Jang, Eung Soo Kim, Hun Sik Kim, Jin-San Yoon

Department of Polymer Science and Engineering, Inha University, Incheon 402-751, Korea

Received 25 July 2003; accepted 18 February 2004
DOI 10.1002/app.22246
Published online in Wiley InterScience (www.interscience.wiley.com).

ABSTRACT: Polypropylene (PP)/montmorillonite (MMT) nanocomposites were prepared by the esterification of propylene-*g*-maleic anhydride (MAPP) with MMT modified with α,ω-hydroxyamines. The structural characterization confirmed the formation of ester linkages and the interaction between the silicate layers. In particular, X-ray diffraction patterns of the modified clays and MAPP/MMT composites showed 001 basal spacing enlargement as great as 0.14–0.62 nm according to the type of α,ω-hydroxyamine. Thermal characterization by thermogravimetric analysis for the composites revealed increased onset temperatures of thermal decomposition. The melting peak temperature decreased, and the crystallization peak temperature increased; this indicated that MMT retarded the crystallization of MAPP. Compounding PP with MAPP/MMT composites enhanced the tensile modulus and tensile strength of PP. However, the elongation at break decreased drastically even when the MMT content was as low as 0.4–2.0 wt %. © 2005 Wiley Periodicals, Inc. J Appl Polym Sci 98: 1229–1234, 2005

Key words: nanocomposites; organoclay; poly(propylene) (PP)

INTRODUCTION

Polypropylene (PP) exhibits an attractive combination of low cost, low weight, and extraordinary versatility in terms of properties, applications, and recycling.[1] To improve the competitiveness of PP in engineering resin applications, it is important to simultaneously increase the dimensional stability, stiffness, strength, and impact resistance. Therefore, special emphasis is being placed on the development of nanofilled PP by means of inorganic–organic nanocomposites.

In recent years, organic–inorganic nanocomposites have attracted great interest because they frequently exhibit unexpected hybrid properties synergistically derived from two or more components.[2–24] Some of the most promising composite systems are hybrids based on organic polymers and inorganic clay minerals composed of layered silicates. A lot of research has been devoted to improving the performance of hybrids by compounding with a few weight percent of nanosized silicates.

The most commonly used clay is the smectite group mineral montmorillonite (MMT), which belongs to the general family of 2 : 1 layered silicates. Their structures consist of two fused silica tetrahedral sheets sandwiching an edge-shared octahedral sheet of either aluminum or magnesium hydroxide.[25] The silicate layers are coupled through relatively weak dipolar interactions and the van der Waals force. Na^+ or Ca^{2+} residing in the interlayers can be replaced by organic cations such as alkylammonium ions via an ion-exchange reaction to render hydrophilic layered silicates organophilic. Of all of the methods used to prepare polymer/clay nanocomposites, the most versatile and environmentally benign approach is based on intercalation through direct polymer melt compounding.

In this study, propylene-*g*-maleic anhydride (MAPP)/MMT nanocomposites were prepared by the compounding of MAPP with MMT modified with α,ω-hydroxyamines, and PP was melt-compounded with the MAPP/MMT composites. Characterizations of the structures, physical properties, and internal micromorphology of the composite materials were performed, and their results are discussed. Furthermore, a physical picture of intercalation based on the swelling behavior of clays is presented.

EXPERIMENTAL

Materials

The clay used in this study was Na^+-montmorillonite (Na-MMT; Southeastern Clay Co., United States). The cation-exchange capacity of Na-MMT was 92

Correspondence to: J.-S. Yoon (jsyoon@inha.ac.kr).
Contract grant sponsor: Inha University

mequiv/g. PP (weight-average molecular weight = 185,000 g/mol) and MAPP (maleic anhydride content = 5 wt %, melting temperature = 150°C, weight-average molecular weight = 8000 g/mol, weight-average molecular weight/number-average molecular weight = 3.9) was obtained from Honam Petrochemical (Yochun, Korea). Ethanolamine (EA), 2-(2-aminoethoxy)ethanol (AEE), and 5-amino-1-naphthol (AN; Aldrich, St. Louis, MO) and titanium (IV) butoxide were reagent-grade and were used without further purification. The solvents were purified by two simple distillations.

Preparation of organophilic layered silicates

Typically, 30 g of Na-MMT was dispersed in 1 L of deionized water. The temperature was raised to 80°C with gentle stirring. Then, 0.3 mol of the α,ω-hydroxyamines and 0.1 mol of HCl (in the case of EA, H_3PO_4 was used instead of HCl) were added to the mixture, and the mixture was stirred for 60 min. The precipitate was subjected to repeated intensive washing by four cycles of centrifugation and redispersion into water. The resulting silicates were dried at 80°C for 48 h and then ground into 10-μ-sized particles in a ball mill.

Preparation of MAPP/MMT nanocomposites

A 500-mL reactor equipped with a thermometer and a condenser was charged with 300 mL of 1,2,4-trichlorobenzene, and then 15 g of MAPP and 0.3–1.5 g (2–10 wt %) of the modified clay were added. The temperature was then raised to 150°C with gentle stirring. Titanium (IV) butoxide (10 μL) as a catalyst was introduced to the reactor. The reaction was terminated after 24 h by cooling the reaction mixture to room temperature. The product was poured into a large amount of *n*-hexane. The precipitated products were separated and purified by several cycles of centrifugation and redispersion into *n*-hexane. The products were dried under reduced pressure at 80°C.

Blending of MAPP/MMT nanocomposites with pp

PP pellets and MAPP/MMT nanocomposites were melt-blended in a Brabender mixer (PLV151 plasticorder; Duisburg, Germany) at 200°C and 50 rpm for 5 min. The obtained strands were pelletized. Sheets 1 mm thick were made via melt pressing under a hot press (model 2697, Fred S. Carver, Inc.; Wabash, IN) at 200°C and 5 tons.

Polymer characterization

Fourier transform infrared (FTIR) spectra were recorded on a PerkinElmer Spectrum 2000 (Boston, MA) over a wave-number range of 4000–400 cm^{-1}. The variation of the interlayer distance of MMT in the nanocomposites was studied by wide-angle X-ray scattering with a Rigaku DMAX 2500 (Denver, CO). The Cu Kα radiation source was operated at 18 kW. Patterns were recorded by the monitoring of those diffractions appearing in the 2θ range of 2–10° with a scanning rate of 1°/min. The tensile properties of the composites were measured with a Hounsfield Co. H 10KS-0061 (Salfords, England) universal testing machine. Specimens were prepared according to ASTM D 638. The crosshead speed was 50 mm/min. The results of five tests were averaged.

The thermal behavior was analyzed with differential scanning calorimetry (DSC; DSC 7, PerkinElmer; Boston, MA). Each sample was heated to 170°C at a heating rate of 20°C/min under a nitrogen atmosphere. After remaining at 170°C for 1 min, it was cooled to −100°C at −200°C/min. It was reheated to 170°C at 20°C/min, and the second-scan thermogram was obtained. The polymer loading in the nanocomposites was estimated by the measurement of the weight loss during thermogravimetric analysis (TGA). A Dupont 9900 (Wilmington, NC) thermogravimetric analyzer was used. TGA measurements were carried out via the heating of 20 mg of each sample up to 600°C at a heating rate of 20°C/min under a nitrogen atmosphere.

The morphological aspects of the composites were examined with transmission electron microscopy (TEM) to determine the internal micromorphology. A JEOL 200 CX TEM (Tokyo, Japan) instrument, with an acceleration voltage of 200 kV, was used.

RESULTS AND DISCUSSION

Structural and molecular characterization

Na-MMT was modified with EA, AEE, and AN. The resulting organoclays were abbreviated EAMMT, AEEMMT, and ANMMT, respectively. MAPP/MMT nanocomposites were prepared through an esterification reaction between the organoclays and MAPP.

IR spectra of the organoclays [organo montmorillonites (Or-MMTs)] are compared with those of Na-MMT in Figure 1. Peaks at 3630 and 1050 cm^{-1} and those between 600 and 400 cm^{-1} are ascribed to —OH stretching of the lattice water, Si—O stretching, and Al—O stretching, respectively, which are characteristic absorption bands of MMT. In addition to those peaks, Or-MMT exhibits peaks at 3350 cm^{-1} corresponding to —NH_3^+ stretching. The IR spectra of the MAPP/MMT composites are illustrated in Figure 2 along with those of MAPP. The absorption bands at 1865 and 1790 cm^{-1} are due to maleic anhydride units. The peak at 1730 cm^{-1} comes from ester linkages, and

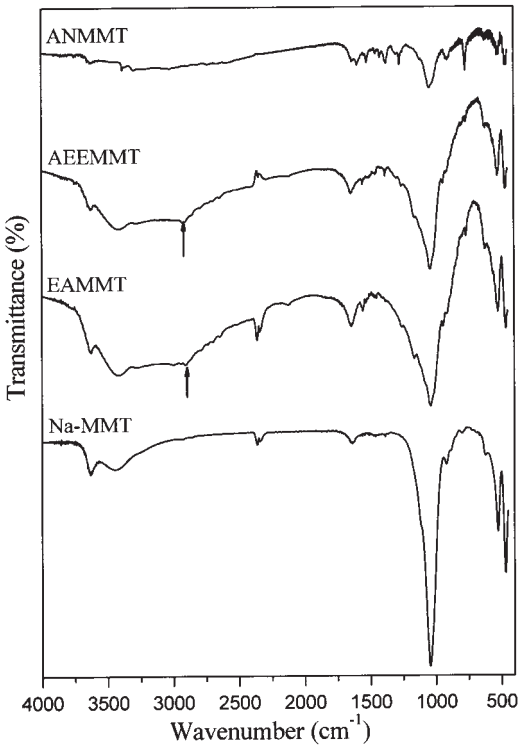

Figure 1 FTIR spectra of Na-MMT and Na-MMT modified with α,ω-hydroxyamines.

the acid carbonyl absorption peak appears at 1710 cm^{-1}. Figure 2 shows that compounding MAPP with Or-MMT decreased the intensity of the anhydride absorption peak. In return, the ester absorption peak became more intense and moved upfield; this indicated that the esterification reaction took place between the anhydride groups of MAPP and the hydroxy groups of Or-MMT.

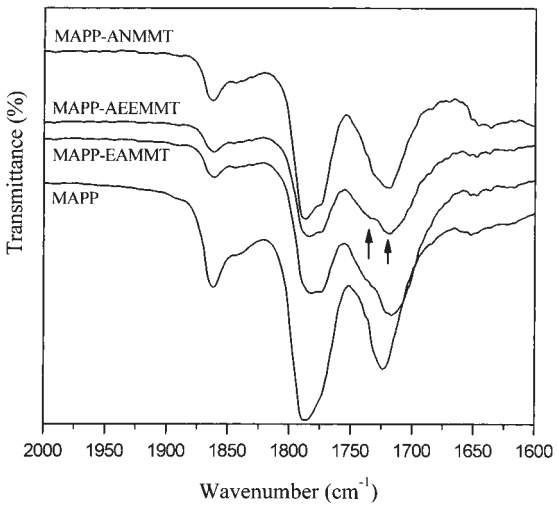

Figure 2 FTIR spectra of MAPP/MMT nanocomposites and MAPP.

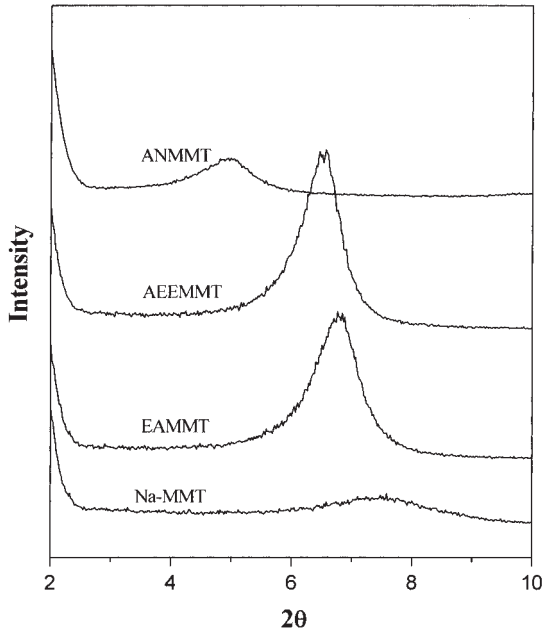

Figure 3 XRD patterns of Na-MMT and Or-MMTs.

Other strong evidence of the intercalation can be obtained from X-ray diffraction (XRD) patterns of Or-MMT and MAPP/MMT composites. Figure 3 shows XRD patterns of Or-MMT and Na-MMT. Or-MMT exhibits a larger interlayer distance than pristine Na-MMT. The interlayer distance increased in the order of Na-MMT $<$ EAMMT $\approx$ AEEMMT $<$ ANMMT.

The XRD patterns of MAPP/MMT composites are shown in Figure 4. Undoubtedly, the overall XRD patterns of the composites are essentially the same as those of Na-MMT, except for the 001 reflection; this indicates that the overwhelming fraction of the composites retains the crystalline structure of MMT. However, the peak corresponding to d_{001}-spacing of Or-MMT and MAPP/MMT composites appears at lower 2θ angles than that of pristine Na-MMT. The interlayer distance calculated from the position of the 001 reflection is listed in Table I. The basal spacing of the composite was enlarged by 0.1–0.6 nm. The spacing distance did not change even when all the Or-MMTs were Soxhlet-extracted with 1,4-dioxane, chloroform, and trichlorobenzene for 24 h; this shows that the organic modifiers were chemically bound between the layers. The three kinds of Or-MMTs were compounded with MAPP. The space was not further enlarged but rather stayed almost invariable when EAMMT and AEEMMT were compounded with MAPP. In the case of ANMMT, the interlayer distance decreased after the compounding with MAPP.

The interlayer distance of MAPP/ANMMT (1.6–1.7 nm), compared with that of Na-MMT (1.17 nm), provides an estimation on the chain conformation of

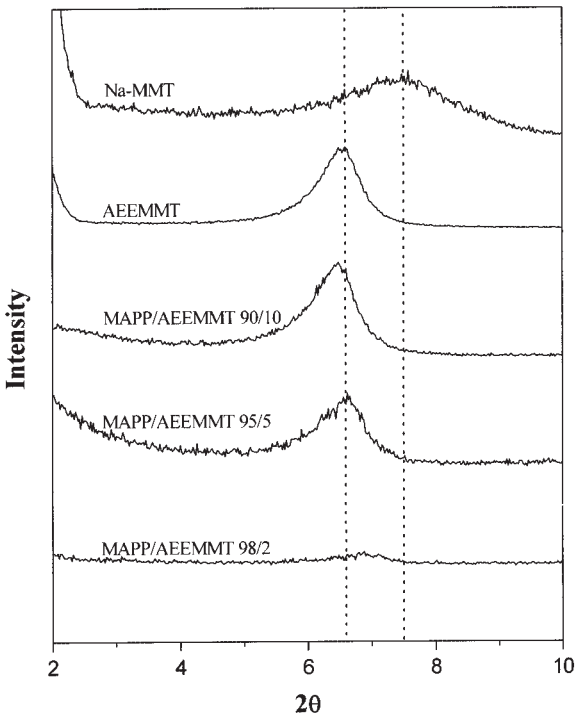

Figure 4 XRD patterns of Na-MMT, Or-MMT, and MAPP/MMT composites.

MAPP intercalated between the layers; that is, MAPP chains run parallel to the interlayers with an extended conformation. Accordingly, MAPP molecules can be intercalated into the interlayers of MMT without further delamination of the ANMMT layers. Therefore, the decreased interlayer distance of ANMMT after compounding with MAPP does not exclude the possibility of a chemical reaction between ANMMT and MAPP. The esterification reaction between MAPP and ANMMT may stretch AN molecules between the silicate layers and, therefore, decrease possibly the interlayer distance of ANMMT.

TABLE I
XRD Data of Or-MMTs and MAPP/MMT Composites

Sample code	Interlayer distance (nm)	Distance increment (nm)
Na-MMT	1.17	—
EAMMT	1.31	0.14
AEEMMT	1.34	0.17
ANMMT	1.79	0.62
MAPP/EAMMT 98/2	1.30	0.13
MAPP/EAMMT 95/5	1.35	0.18
MAPP/EAMMT 93/7	1.29	0.12
MAPP/EAMMT 90/10	1.34	0.17
MAPP/AEEMMT 98/2	1.28	0.11
MAPP/AEEMMT 95/5	1.33	0.16
MAPP/AEEMMT 93/7	1.32	0.15
MAPP/AEEMMT 90/10	1.36	0.19
MAPP/ANMMT 98/2	1.69	0.52
MAPP/ANMMT 95/5	1.58	0.41
MAPP/ANMMT 93/7	1.61	0.44
MAPP/ANMMT 90/10	1.68	0.51

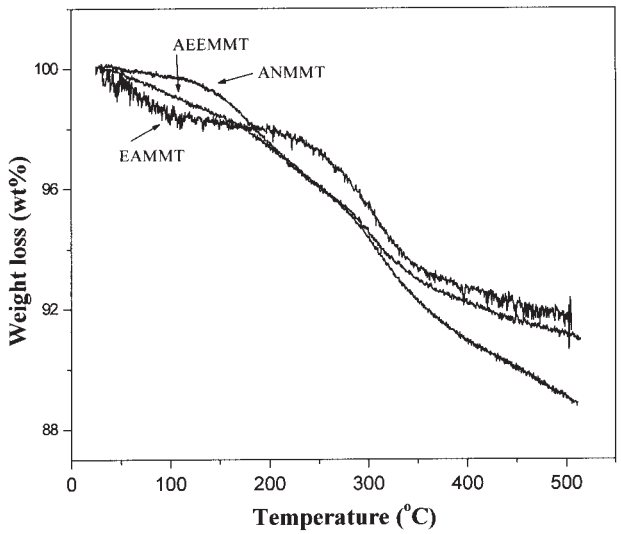

Figure 5 TGA thermograms of Na-MMT modified with α,ω-hydroxyamines.

Thermal characterization

The clay content of the composites was determined from the residual content after TGA, as shown in Figure 5. The content of organic components in the MAPP/MMT composites was also determined from

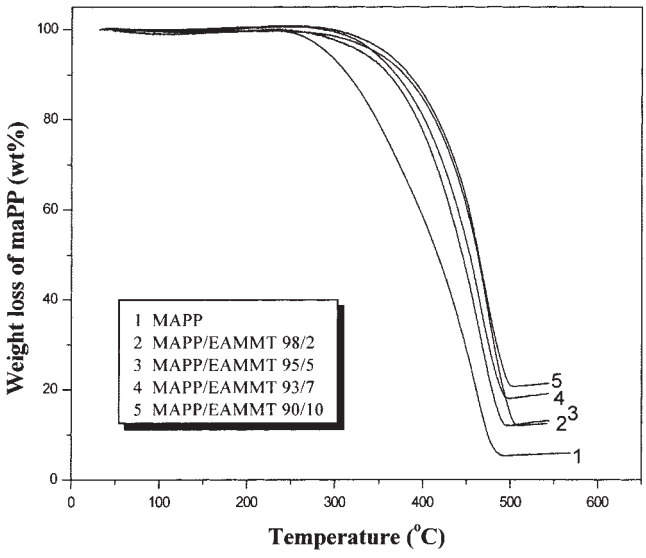

Figure 6 TGA thermograms of MAPP and MAPP/MMT nanocomposites.

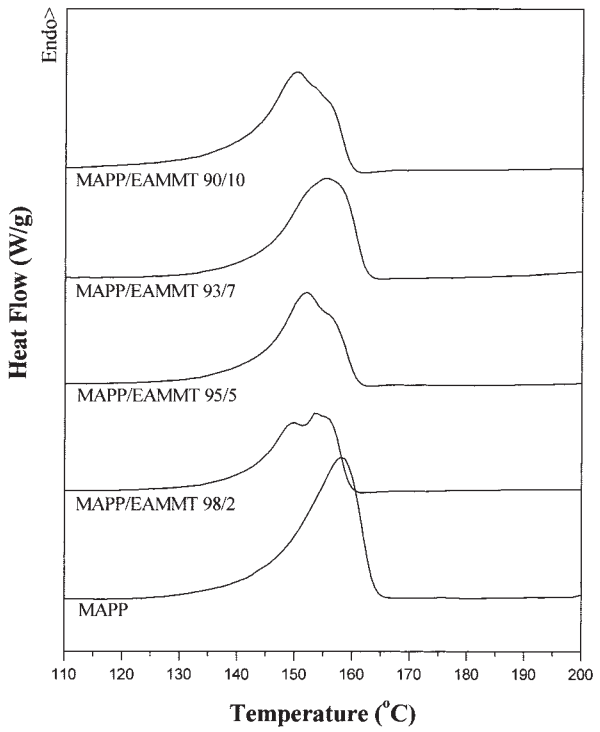

Figure 7 DSC thermograms of MAPP and MAPP/EAMMT nanocomposites.

the weight loss during TGA, as demonstrated in Figure 6. The onset temperature of the weight decrease in TGA moved to a higher temperature region as the content of MMT in the composites increased. This enhancement of the thermal stability indicates that the MAPP/MMT composites were not simple blends but that MAPP was molecularly compounded with MMT.

DSC traces of MAPP/EAMMT are shown in Figure 7 together with those of MAPP. The melting peak temperature of the MAPP domain observed during the reheating step after quenching from the molten state decreased with an increase in the content of EAMMT. This is attributed to the fact that EAMMT seizes firmly the chemically bound MAPP molecules to suppress the crystallization of MAPP.

Mechanical properties of PP blended with MAPP/MMT composites

The tensile properties of MAPP/MMT nanocomposites blended with PP are summarized in Table II. The MAPP/MMT composites had a powdery texture and were not easily molded alone to prepare specimens for the tensile tests. Instead, PP was melt-blended with the MAPP/MMT composites. The tensile modulus and tensile strength of PP were marginally enhanced as a result of the blending with MAPP/MMT. The enhancement of the modulus can be ascribed to the resistance exerted by MMT layers against plastic deformation of the polymer. In addition, the stretching resistance of polymer chains with an extended conformation in the gallery also contributed to the modulus enhancement.[19–21] However, the elongation at break decreased drastically even when the concentration of MMT was as low as 0.4–2.0 wt %.

MAPP molecules in MAPP/MMT composites should have loop conformations because all the anhydride units on MAPP can react with the hydroxyl groups of Or-MMT with equal probability. The loop structure of MAPP with a relatively low weight-average molecular weight makes the chain entanglement of MAPP with PP practically implausible. Therefore, an interaction between PP and MAPP/MMT should be principally due to the van der Waals force. Further research is required to compound Or-MMT with high-molecular-weight MAPP. For this purpose, a special

TABLE II
Mechanical Properties of 20 Parts of MAPP/MMT Nanocomposites Blended with 80 Parts of PP

Sample code	Clay content (wt %)	Tensile strength (MPa)	Elongation (%)	Tensile modulus (MPa)
PP	0	29.2 ± 2.3	715.6 ± 98.3	1078 ± 233
MAPP	0	20.0 ± 4.4	43.0 ± 11.3	974 ± 172
MAPP–PP 20/80[a]	0	28.2 ± 1.5	329.7 ± 67.3	1102 ± 166
EAMMT–MAPP–PP[b]	0.4	30.7 ± 1.9	3.4 ± 1.6	1302 ± 241
EAMMT–MAPP–PP[b]	1	32.6 ± 0.9	4.2 ± 0.9	1117 ± 118
EAMMT–MAPP–PP[b]	1.4	31.5 ± 4.4	4.4 ± 0.4	1451 ± 153
EAMMT–MAPP–PP[b]	2	31.7 ± 2.5	3.7 ± 1.8	1228 ± 139
AEEMMT–MAPP–PP[b]	0.4	30.6 ± 2.2	3.6 ± 1.3	1267 ± 203
AEEMMT–MAPP–PP[b]	1	29.2 ± 2.5	3.3 ± 1.7	1235 ± 138
AEEMMT–MAPP–PP[b]	1.4	30.4 ± 2.0	4.0 ± 1.2	1315 ± 168
AEEMMT–MAPP–PP[b]	2	31.6 ± 3.1	4.5 ± 1.3	1258 ± 133
ANMMT–MAPP–PP[b]	0.4	30.3 ± 5.7	4.0 ± 1.1	1245 ± 214

[a] PP was melt-blended with MAPP at a weight ratio of 20/80 MAPP/PP.
[b] PP was melt-blended with MAPP/MMT composites.

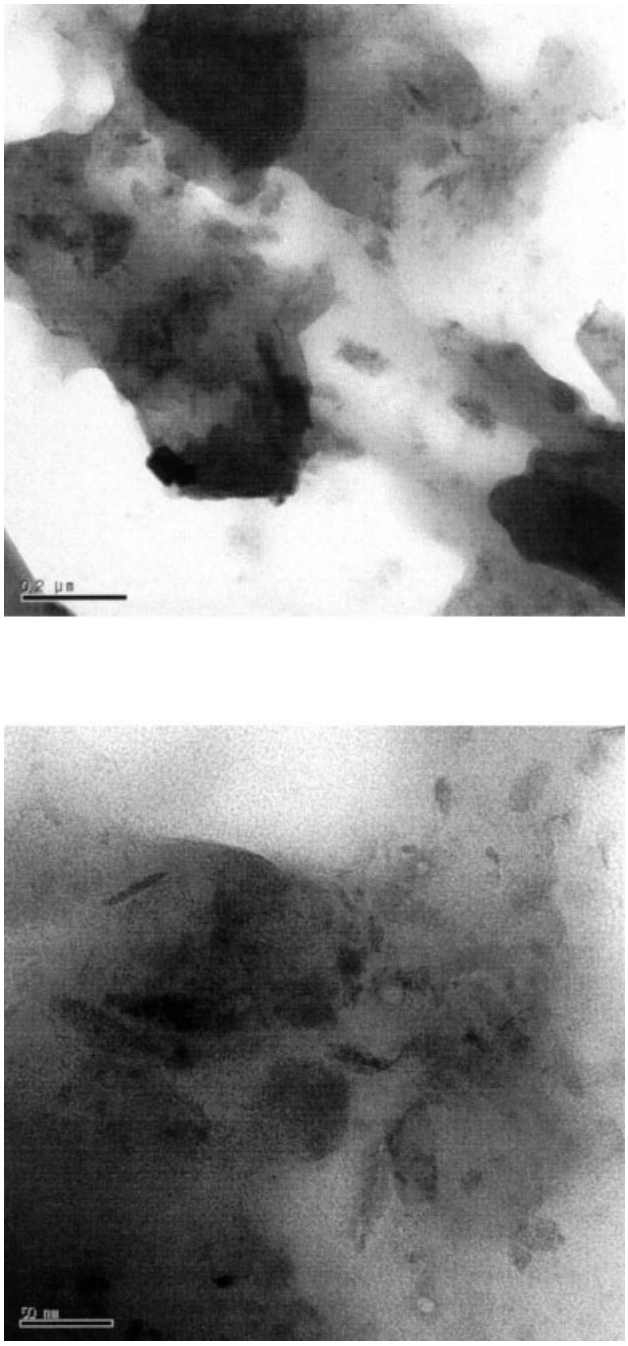

Figure 8 TEM micrographs of nanocomposites (95/5 MAPP/ANMMT).

synthesis scheme should be devised because the grafting of maleic anhydride units onto PP by peroxides is usually accompanied by chain scission of PP molecules.

Morphology of the mapp/mmt composites

The morphology of the composites was examined with TEM to observe the dispersion state of the silicate layers. Figure 8 shows TEM micrographs of 95/5 MAPP/ANMMT and demonstrates that 1–2-nm silicate layers were arranged in good order and were well dispersed in the polymer matrix.

References

1. Moore, E. P. Polypropylene Handbook; Hanser: Munich, 1996.
2. Giannelis, E. P. Adv Mater 1993, 8, 29.
3. Krishnamoorti, R.; Giannelis, E. P. Macromolecules 1997, 30, 4097.
4. Vaia, R. A.; Giannelis, E. P. Macromolecules 1997, 30, 8000.
5. Balazs, A. C.; Singh, C.; Zhulina, E. Macromolecules 1998, 31, 8371.
6. Lyatskaya, Y.; Balazs, A. C. Macromolecules 1998, 31, 6676.
7. Novak, B. M. Adv Mater 1993, 6, 422.
8. Lu, S.; Melo, M. M.; Zhao, J.; Pearce, E. M.; Kwei, T. K. Macromolecules 1995, 28, 4908.
9. Usuki, A.; Kawasumi, M.; Kojima, Y.; Fukushima, Y.; Okada, A.; Kurauchi, T.; Kamigaito, O. J Mater Res 1993, 8, 1179.
10. Kojima, Y.; Usuki, A.; Kawasumi, M.; Fukushima, Y.; Okada, A.; Kurauchi, T.; Kamigaito, O. J Mater Res 1993, 8, 1185.
11. Kojima, Y.; Usuki, A.; Kawasumi, M.; Fukushima, Y.; Okada, A.; Kurauchi, T.; Kamigaito, O. J Polym Sci Part A: Polym Chem 1993, 31, 1755.
12. Wang, M. S.; Pinnavaia, T. J. Chem Mater 1994, 6, 468.
13. Lan, T.; Pinnavaia, T. J. Chem Mater 1994, 6, 2216.
14. Kelly, P.; Akelah, A.; Qutubuddin, S.; Moet, A. J Mater Sci 1994, 29, 2274.
15. Vaia, R. A.; Isii, H.; Giannelis, E. P. Chem Mater 1993, 5, 1694.
16. Moet, A.; Akelah, A. Mater Lett 1993, 18, 97.
17. Messersmith, P. B.; Giannelis, E. P. J Polym Sci Part A: Polym Chem 1995, 33, 1047.
18. Biasci, L.; Aglietto, M.; Ruggeri, G.; Ciardelli, F. Polymer 1994, 35, 3296.
19. Lee, D. C.; Jang, L. W. J Appl Polym Sci 1996, 61, 1117.
20. Lee, D. C.; Jang, L. W. J Appl Polym Sci 1998, 68, 1997.
21. Jang, L. W.; Kang, C. M.; Lee, D. C. J Polym Sci Part B: Polym Phys 2001, 39, 719.
22. Kawasumi, M.; Hasegawa, N.; Kato, M.; Usuki, A.; Okada, A. Macromolecules 1997, 30, 6333.
23. Hasegawa, N.; Kawasumi, M.; Kato, M.; Usuki, A.; Okada, A. J Appl Polym Sci 1998, 67, 87.
24. Kato, M.; Usuki, A.; Okada, A. J Appl Polym Sci 1997, 66, 1781.
25. Whittingham, M. S.; Jacobson, A. E. Intercalation Chemistry; Academic: New York, 1982.